Effect of Pressure on Carbon monoxide Oxidation on Titania Supported Platinum Nanoparticles Catalyst

Jovine Emmanuel

University of Dar es Salaam, Mkwawa University College of Education, Department of Chemistry,, P.O.Box 2513 Iringa-Tanzania

ABSTRACT

Thermographic testing methodology was developed to facilitate measurements of particle dimension and substrate influence in heterogeneous catalysts. A screening chip with several areas of less stress silicon nitride membranes which displays less heat conductivity and heat capacity was used. Heat produced during the reaction on catalysts deposited on membranes was established through IR camera which gave the value of the turn over frequency. Effect of pressure on CO conversion on titania supported Pt particles of different dimension was measured on 120 catalysts concurrently. The reaction was studied at various O_2 and CO pressures at 170 and 240 . At these temperature conditions, activity increased with increase of O_2 and CO pressure, in agreement with previous reports.

INTRODUCTION

There is a fair idea on catalysis from ancient times. It largely contributes in a number of applications as in chemical and pharmaceutical industry, and energy transformation and environmental safety (Scheidtmann *et al*., 2001, Emmanuel, 2022). Estimates indicate that above 90% of chemical production routes depend on a single or multiple catalytic pathways (Armor, 2011, Emmanuel and Hayden, 2022). Metal catalysts largely rely on substrate, shape and dimension of supported metal nanoparticles catalyst. Reports indicate that the reactivity of properly characterised supported catalysts are important in knowing the influence of particle dimension and substrate. A good case of such a catalyst revealing a greater substrate and particle dimension influence on reactivity is supported platinum (Pt) in low temperature conversion of tiny molecules like carbon monoxide (CO) and hydrocarbons (Liu *et al*., 2010). Platinum (Pt) is among the frequently used metal catalysts in enormous applications over the decades. Dobereiner reported the activity of Pt in 1800s where it was applied in the catalysis of H_2 and

O_2 in portable lamp (Somorjai, 1994). Besides, Pt related catalysts are applied in different reactions such as the transformation of aliphatic straight-chain organic molecules to aromatic molecules and branched molecules, in huge scale hydrogenation in chemical and petroleum-refining industries and ammonia conversion (Somorjai, 1994). More significantly, it is used for CO oxidation and unburned hydrocarbons in car emissions control (Franceschetti *et al*., 2003). Platinum catalyst, on the other hand, is the most commonly applied and active electrode in fuel cell technology (Franceschetti *et al*., 2003). Although Pt is widely used in various fields, it is an expensive precious metal and less abundant which make its application in various technologies largely challenging (Cameron *et al*., 2003). Because Pt bare high cost, the priority has been its application at the atomic scale in heterogeneous catalysis. This includes the spreading of Pt particles on high surface area metal oxide substrates like Al_2O_3, TiO_2 and Fe_2O_3 which reduce the quantity of Pt integrated in the catalyst (Somorjai, 1994). Supporting Pt lowers the catalyst expenses in addition to increasing effective surface area of the catalyst in addition, it strengthens catalyst' particles. Substrates like TiO_2 are directly involved in reaction pathways through reactants and intermediates activation thus, improving the activity. Pt catalysts on carbon is widely applied in PEMFCs technology (Emmanuel, 2022). However, application of Pt catalyst is affected because of the decline of catalytic efficiency due to particle disintegration, rusting of cathode substrate and CO inhibition (Kim and Jhi, 2011). The decline of efficiency is because of greater interaction of Pt and CO which inhibits O_2 from getting on the surface of a catalyst (Schubert *et al*., 2001; Molina *et al*., 2009; Liu

et al., 2010). Carbon monoxide conversion reaction on Pt supported catalysts is widely investigated (Santra and Goodman, 2002; Liu *et al*., 2010; Slavinskaya *et al*., 2011; Allian *et al*., 2012; Dobrin, 2012). It is known that because of strong interaction with oxygen and Pt surface, O_2 adsorbs and break down to generate effective surface adsorbed atomic oxygen which combines with adsorbed CO to generate CO_2 (Bamwenda *et al*., 1997; Haruta, 2003; Gao *et al*., 2009). Carbon monoxide conversion on Pt proceeds very efficiently with a conversion rate dependent on CO and oxygen partial pressures. Previous reports show that the reaction needs chemisorbed oxygen and CO on Pt surface, a pathway termed as Langmuir-Hinshelwood mechanism (McCash, 2001; Kolasinski:, 2002; McClure and Goodman, 2009; Liu *et al*., 2010, Santos *et al*., 2010). Studies indicate that this reaction is influenced by reactants pressure, coverage and surface temperature (Kolasinski:, 2002). However, competitive adsorption among CO and O_2 is reported. Although CO can adsorb on an O_2 occupied surface, O_2 cannot adsorb on CO occupied surface. With high CO occupied surface, the reaction is restricted by O_2 thus, raising CO pressure inhibits the reaction because no extra adsorption sites for O_2. However, at low CO occupancy, O_2 adsorption proceeds rapidly and the reaction relies on surface coverage of CO and O_2 (Kolasinski:, 2002). Given the catalytic efficiency of Pt catalyst, the reactivity is hampered by CO inhibition in gas-phase CO oxidation thus, maximum CO oxidation to CO_2 is attained at minimal CO surface occupancy (McClure and Goodman, 2009). In this regards, Pt catalysts on substrates are perceived as poor catalysts for small temperature CO conversion (Li *et al*., 2008).

Studies indicate that Fe_2O_3 supported Pt nanoparticles catalyst exhibits unusual high catalytic properties for CO conversion at small temperature (Liu *et al*., 2010). The activity is associated with the capability of Fe_2O_3 to provide active oxygen during the reaction. Titania supported Pt nanoparticles less than 5 nm show low activity for CO oxidation reaction (Rashkeev *et al*., 2007). Theoretical studies propose that Pt nanoparticles between 1 and 2 nm dimensions are more effective for CO oxidation (Dobrin, 2012). Further reports indicate that Pt particles of 2 nm dimension are the best effective for CO conversion in comparison with those of 3 nm and 5 nm dimensions (Kageyama *et al*., 2013). Whereas the combinatorial creation of properly characterised oxide supported metal nanoparticle electrocatalysts enabled the testing of various electrochemical reactions on different substrates using a high throughput electrochemical chip, the use of high throughput test for heterogeneous catalysts reactions is a bit complex. Well-designed approach appropriate for thin film small area alloy catalysts was revealed for H_2-D_2 exchange reaction using a 100 channel microreactor array and mass spectroscopy (Emmanuel *et al*., 2019). For less complex reactions in which it is not important to establish selectivity, net activity established in the heat generating reaction through infrared thermography methodology is promising. This methodology was applied for testing of catalysts in the conversion of hydrogen and octane on high area catalyst samples (Emmanuel *et al*., 2019). However, expansion of the methodology to arrays of properly characterised catalysts like metal supported electro-catalysts to achieve structure/activity influences is a challenge (Hayden, 2013). The considerably low surface area of planar catalysts needs an amplified sensitivity so as to identify the heat produced in the course of a reaction. The current study reports the impact of pressure on reactivity of titania supported Pt particles catalyst for CO conversion by applying a nano-fabricated screening chip which enables simultaneous testing of a chains of supported Pt catalysts of controlled particle dimension at different CO and O_2 pressures.

MATERIALS AND METHODS

Creation of platinum nanoparticles catalysts

A combinatorial technique centred on a high throughput physical vapour deposition (HT-PVD) developed by Brian et al. (Hayden et al., 2009) was used to create thin films of TiO_2 and TiO_2 supported Pt nanoparticles catalyst, Figure 1.
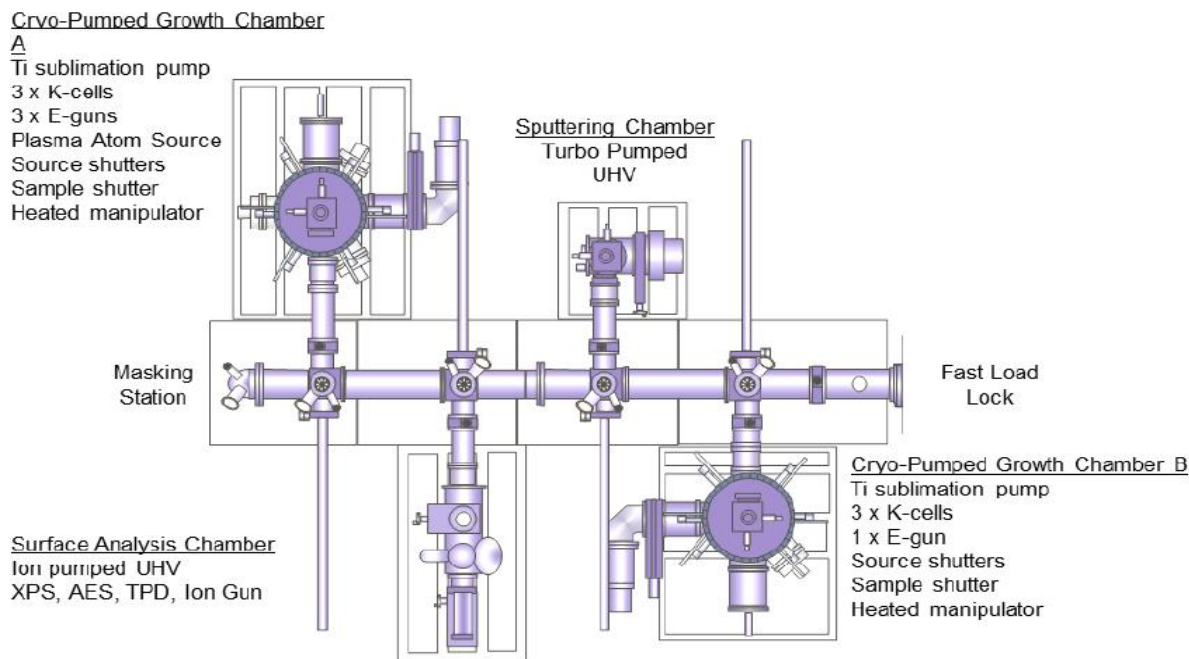
Figure 1: Schematic diagram of HT-PVD system indicating two cryo-pumped thin film synthesis chambers A and B, sputtering and surface analysis chambers and the load lock (adapted from Hannah, 2012).

This technique creates thin films through condensation of evaporated material onto a substrate. The deposition chamber consisted of three electron gun (e-gun) evaporation sources (Temescal) and three Knudsen cell (K-cell) sources (DCA). The HT-PVD system operational base pressure was 1×10^{-10} mbar. In the present study, electron beam sources, E-gun 1 was applied to evaporate Ti, Pt was evaporated from E-gun 3. Titania layers of about 200 nm were deposited onto a catalyst screening chip from titanium (99.995 %, Alfa Aesar metals) from E-gun 1 and oxygen (Air products, special gases, 99.999 %) at a constant pressure of 9.7×10^{-6} Torr at 1 sccm oxygen flow rate and plasma source, $P_{rf} = 300$ W at a deposition rate of 4 Å/s with substrate retained at ambient temperature throughout film creation.

The widths of titania layer deposits were managed through deposition time and sample thickness was subsequently achieved via calibration of deposition rates from AFM readings. The AFM (Vecco Autoprobe M5) instrument was applied in a contact mode with a silicon cantilever, resonance frequency of 180 kHz, spring constant of 5Nm^{-1} with an estimate tip (CSC17 probe, MikroMasch) curvature of 10 nm.

Characterization of platinum nanoparticles

Characterization and distribution of particle dimension was conducted by using TEM where a small layer of TiO$_2$, 15-25 nm thick, was created onto small carbon coated copper TEM grids (Agar scientific). The grids bared TiO$_2$ produced under the same deposition conditions as a catalyst screening chip. Platinum particles

from Pt source (E-gun 3), were created onto a screening chip where TiO_2 support material was previously created through HT-PVD technique. The deposition rate of 4 Å/s were achieved by creating several thick layers from short to extended times, showing that the thickness as established on contact masked samples using AFM was relative to the deposition duration. The rate of Pt deposition (0.15 Å/s) was established through creation of continuous Pt small films, and reduced deposition durations (30 s – 360 s) applied to create Pt particles via nucleation and growth on titania substrates at 250 . For surface characterization of Pt nanoparticles on titania substrate, Pt nanoparticles were grown onto Formvar® carbon coated copper grids (Agar scientific) coated with a small layer of titania 15-25 nm thick for transmission electron microscope (TEM) measurements. Characterization of particles was conducted by TEM prior deposition onto the screening chip for assurance of particles creation. The TEM images were attained by using Jeol 3010 instrument at an accelerating voltage of 300 kV containing a Gatan CCD camera for capturing images. X-ray Photoectron Spectroscope (XPS) studies were conducted in Ultra High Vacuum (UHV) system containing a twin anode X-ray source (Mg K and Al K) and a VG Clam Single Channel XPS system analyser. Depositions were undertaken onto silicon nitride on silicon and on a 10 x 10 or 12 x 12 array nano-fabricated catalyst screening chip (450 µm silicon wafer thickness) on which a low pressure chemical vapour created (LP-CVD) silicon nitride membrane (300 nm and 600 nm) has been previously created. The screening chip was back etched to create individual membranes. The HT-PVD system was set up on a "wedge" deposition to

generate different particle dimensions distributions throughout the support.

A silicon chip with the dimension of 35 mm x 35 mm was fabricated (450 mm thick silicon wafer) for IR thermography readings and an array of 10 x 10 silicon nitride membranes (1.5 mm x 1.5 mm) of 600 nm thickness were produced by back etching of silicon to a layer of LP-CVD silicon nitride as described earlier (Emmanuel, 2022). The membrane with 200 nm of titania substrate was optically transparent. For temperature measurement of the membrane, a small graphitic carbon layer (ca. 200 nm) was created on the back of the membrane supplying an emissivity approximate to that of a black body. Thin SiN membrane offered a support for the catalyst with small thermal mass and less thermal conductivity to the surrounding silicon chip thus, heat produced in the course of a reaction on the catalyst could subsequently increase membrane temperature.

Testing of platinum nanoparticles for catalytic activity

A screening chip with a catalyst created on the whole chip was placed on a heated sample holder with a heat shield to enable the whole chip to be heated evenly up to 250 °C. The sample holder was placed in a UHV system an IR transparent window (CaF_2) and the surface of the chip was captured (50 mm focal length camera lens) by a thermal camera (Jade III, CEDIP) operating in the spectral range of 3.6 – 5.1 µm with a thermal sensitivity of 20 mK.

Spatial resolution was 320 x 240 pixels and the whole 12 x 12 array was imaged to fill the detector. Reactions were conducted in a turbomolecular pumped UHV system with a

base pressure of 1 x 10^{-10} mbar and the temperature response of the catalyst on the membrane for a given power input (from an exothermic reaction) was established via finite element thermal modelling (Comsol Multiphisics$^®$) (Emmanuel, 2022).

The supposition is that the energy wasted above the membrane could be via conduction through the membrane (together with titania support and the graphite layer) to the supporting silicon chip. Radiative and convective losses were estimated to be zero therefore, extra radiative and convective wastes over a few degrees temperature over the base temperature of reaction were expected to be very minimal (Emmanuel, 2022). For CO conversion reaction (H = -283 kJmol^{-1}) (Emmanuel, 2022) and a pressure of 1 x 10^{-3} mbar, assuming each molecule is converted, the theoretical power was 2.289 x 10^{-4} Js^{-1} mm^{-2} (Emmanuel, 2022). This leads to a calculated temperature increase at the centre of the membrane, T = 4 . The calculated sensitivity of the chip allowed the determination of turn over frequency (TOF) of reaction at the surface such that the error attributed to the absolute value of the TOF were approximated to be +/- 30% due to uncertainties in the thermal conductivity values for the membrane composite layer. A simulation of the temperature distribution throughout the 1.5 mm x 1.5 mm membrane has been reported earlier (Emmanuel, 2022).

RESULTS AND DISCUSSION

Images of TEM for Pt catalyst supported on titania resemble those reported earlier in terms of their shape and growth mode (Emmanuel, 2022), Figure 2. The TEM images facilitated the determination of particle dimension reliance of supported Pt in relative to the equivalent coverage of Pt created. On the Figure, particles of Pt appear in black relative to the white substrate background. At a shorter deposition period (30 seconds) in (a), particles are smaller (black). Conversely, when deposition periods escalate, particles increase in dimension because extra Pt is being added as witnessed in the dimension of particles in (b), (c) and (d), respectively, with deposition periods of 30 seconds, 2, 3.5 and 5 minutes, respectively.

In order to establish the change of particle dimension distribution after CO conversion because it was not possible to have it established directly on the chip by TEM, XPS measurements were conducted prior and after the reaction. A small change to higher binding energy was observed which was associated with final-state effect, consistent with earlier studies (Liu *et al*., 2014). The raise in the intensity was detected with increasing particle dimension, showing that Pt particles were growing in size as extra Pt was deposited. The study of Pt core level energies show a small but recognizable shift in binding energy.

Studies indicate that the binding energy shifts governed by the species to which an atom is attached and the binding energies shifts for core level electrons can emerge from initial-state or final-state effects (Attard and Barnes, 1998, Kolasinski:, 2002).
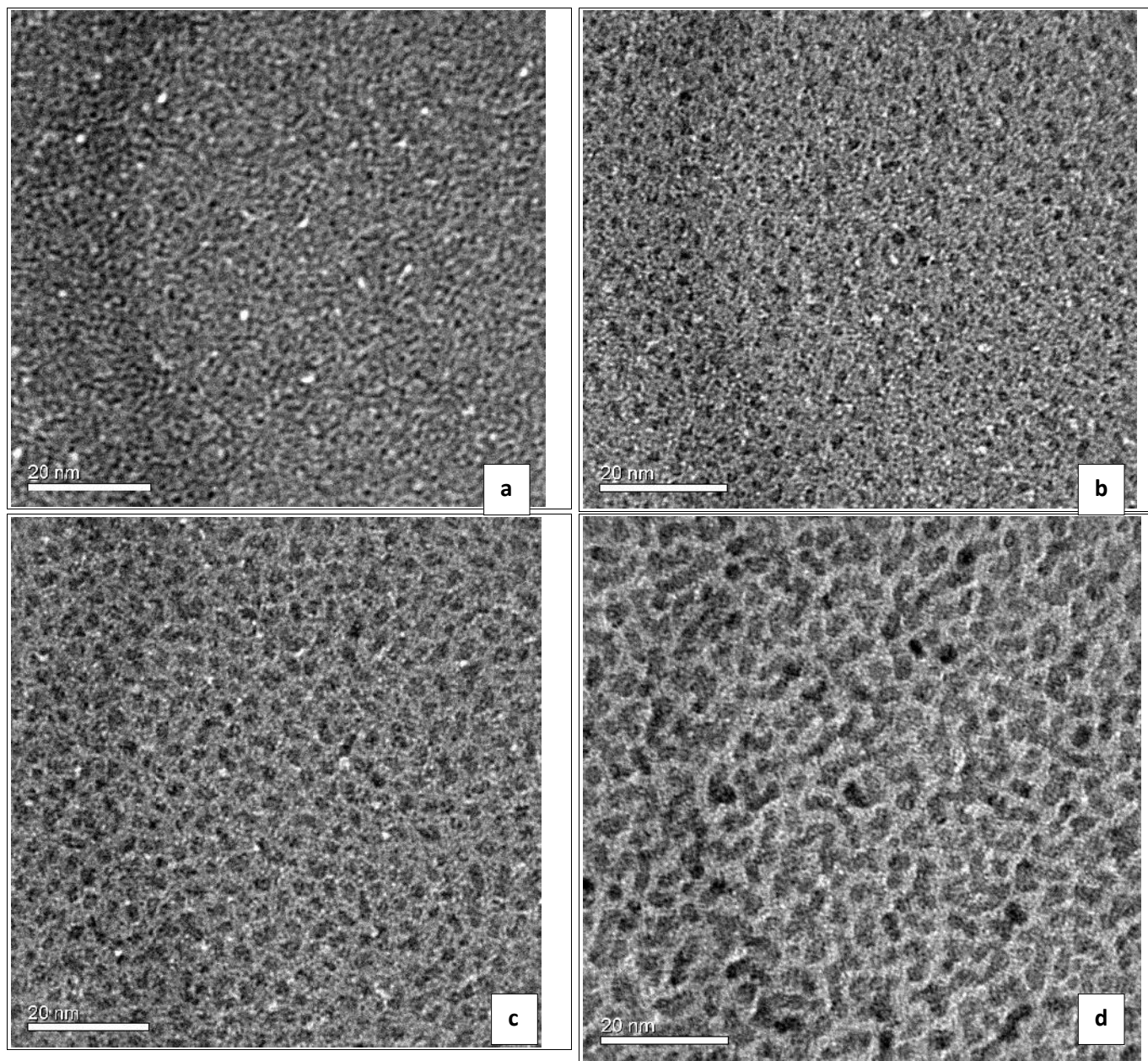
Figure 2: Images of TEM for Pt particles at different deposition periods, (a) 30 seconds, (b) 2 minutes, (c) 3.5 minutes and (d) 5 minutes with a mean particle dimension of (a) 1.6 nm, (b) 2.6 nm, (c) 4.9 nm and (d) 6.7 nm

Initial-state effects (chemical shift) are attributed to chemical bonding which largely affects electronic configuration of an atom leading into a large shift in binding energy of up to 10 eV (Emmanuel, 2022). Thus, atoms in a high oxidation state generate XPS peaks at high binding energy as compared to similar atom in a low oxidation state (Emmanuel, 2022). However, the final-state effects are because of the ejection of an electron from an atom which

corresponds to an ionic state producing a hole in place of the removed photoelectron (Emmanuel, 2022). Effect of the binding energy shift due to final-state is often a slight binding energy shift compared to that of initial-state effect. Because the core level binding energy shift for Pt particles detected in the current study is smaller,

typically less than 1 eV, it can be linked with final state-effect, consistent with the earlier reports (Zhang *et al*., 1997; Guerin *et al*., 2006; Liu *et al*., 2014,). Figure 3 show the reliance of Pt $4f_{7/2}$ binding energy for Pt particle dimension recorded on the screening chip prior and after the reaction on Pt supported catalysts.
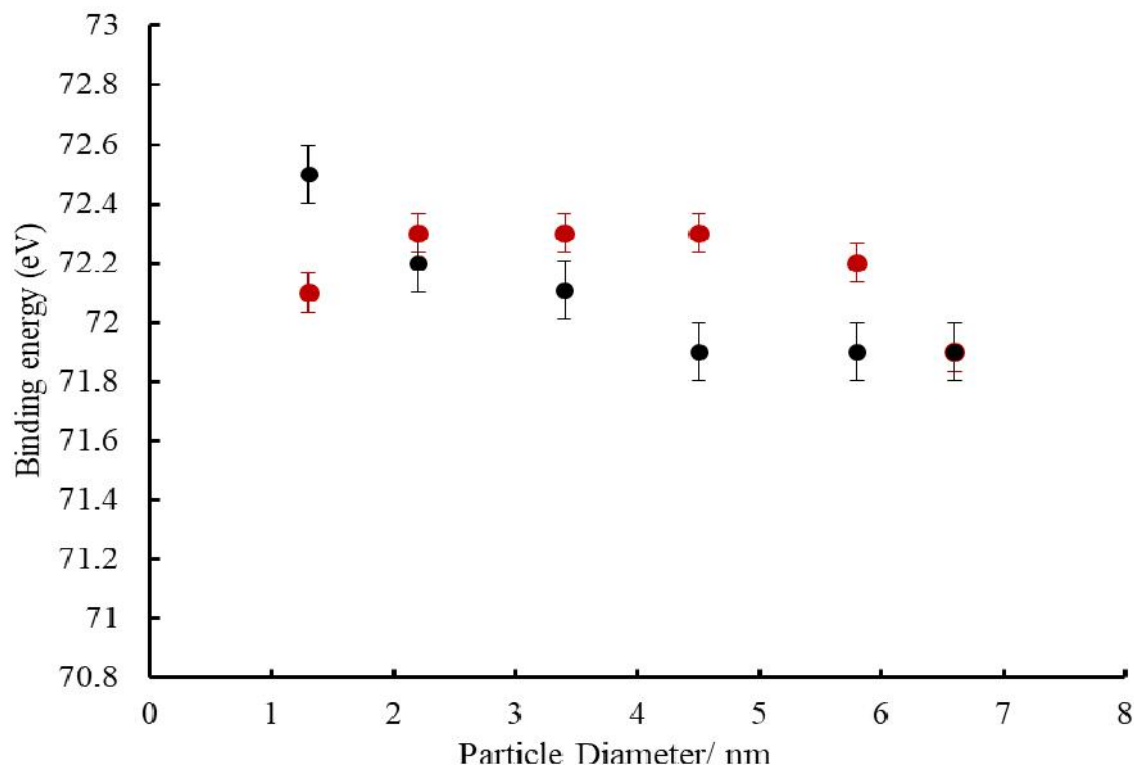

Figure 3: Binding energy of Pt particle size for the Pt 4f7/2 prior and after the catalytic reaction.

At a base temperature of 170 $^{\circ}$C on Pt catalyst, a pressure of a gaseous mixture was 7.2×10^{-2}, 8.4×10^{-2} and 1.04×10^{-1} mbar with O_2: CO ratio of 1:1. For a pre-exposed O_2 catalyst surface, the pressure was 1.5×10^{-1}, 1.9×10^{-1} and 2.2×10^{-1} mbar with O_2: CO ratio of 2:1, 1:1 and 1:1, respectively, while on a pre-exposed CO catalyst surface the pressure was 1.5×10^{-1}, 1.7×10^{-1} and 2.2×10^{-1} mbar with O_2: CO ratio of

1:2, 1:1 and 1:1, respectively. Besides at 240 and O_2: CO ratio of 1:1, the pressure was 6×10^{-1}, 1.1 and 2.4 mbar.

The temperature was determined concurrently on the catalysts integrating over a 5 minutes interval. Catalysts were created such that particles dimension was constant throughout the rows and differed in the columns of the screening chip. The change in temperature

across a row of similar particle dimensions was 0.2   , far less than that in the columns and was attributed to a partial shielding of the gas flux at the edges of the sample by the holder. The increase,   T, in average was applied to establish the oxidation rate of CO to CO_2 at the catalyst assuming the enthalpy of reaction was   H = -283 kJ mol^{-1} (Emmanuel, 2022). The mass of Pt and number of Pt atoms at the surface of the particles per catalyst area of catalyst was calculated from TEM images, assuming the particles were hemispherical (Hayden *et al*., 2009, Emmanuel, 2022). This allowed the computation of TOF at Pt surface. Figure 4 presents the TOF for CO conversion reaction at 170   with the pressure of 7.2 x 10^{-2}, 8.4 x 10^{-2} and 1.04 x 10^{-1} mbar and O_2: CO ratio of 1:1.
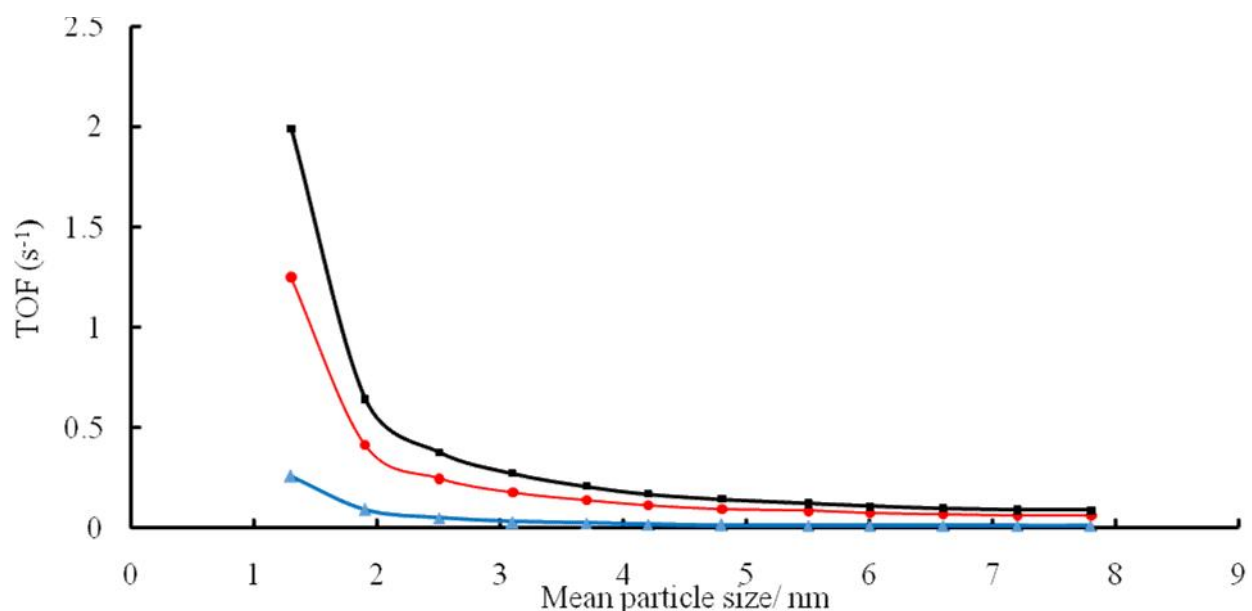

Figure 4: TOF for CO conversion on Pt particles at a pressure of 7.2 x 10^{-2} (blue triangles), 8.4 x 10^{-2} (red circles) and 1.04 x 10^{-1} mbar (black squires) with O_2: CO ratio of 1:1 at 170   .

In Figure 5 is the TOF for CO conversion reaction on a pre-exposed O_2 catalyst surface with a pressure of 1.5 x 10^{-1}, 1.9 x 10^{-1} and 2.2 x 10^{-1} mbar at O_2: CO ratio of 2:1, 1:1 and 1:1, respectively, at 170   . Figure 6 presents the TOF for CO conversion at 170   on a pre-exposed CO catalyst surface with a pressure of 1.5 x 10^{-1}, 1.7 x 10^{-1} and 2.2 x 10^{-1} mbar at O_2: CO ratio of 1:2, 1:1 and 1:1, respectively
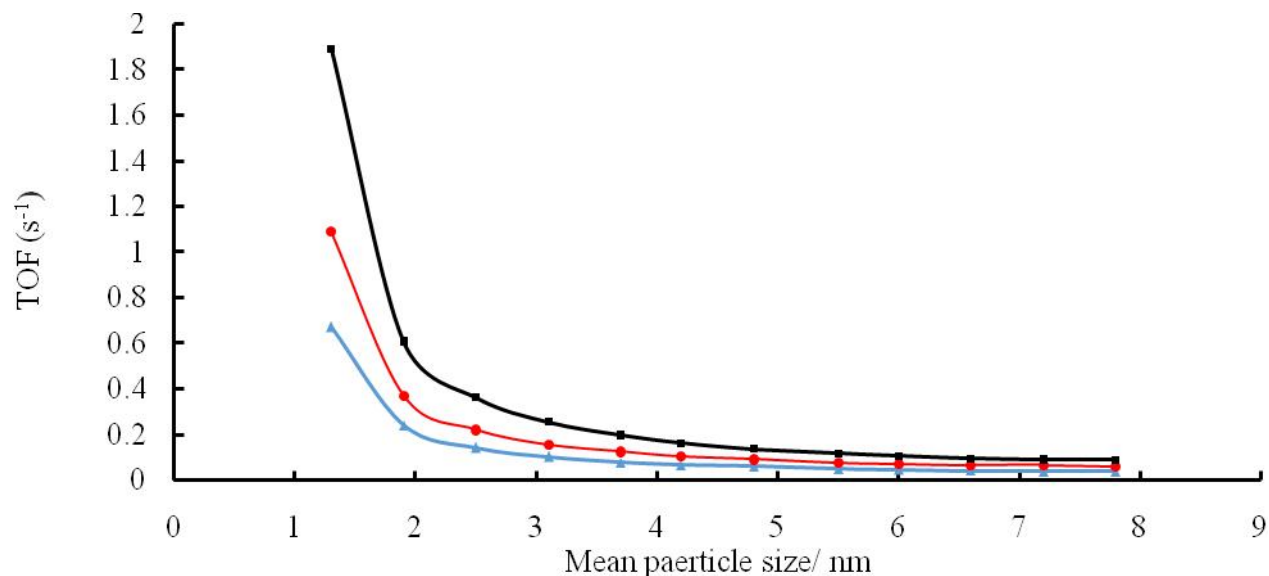
Figure 5: TOF for CO conversion reaction on Pt particles catalyst for a pre-exposed O$_2$ Pt surface, pressure of 1.5 x 10^{-1} (blue triangles), 1.9 x 10^{-1} (red circles) and 2.2 x 10^{-1} mbar (black squires) at O$_2$: CO ratio of 2:1, 1:1 and 1:1, respectively, at 170 .
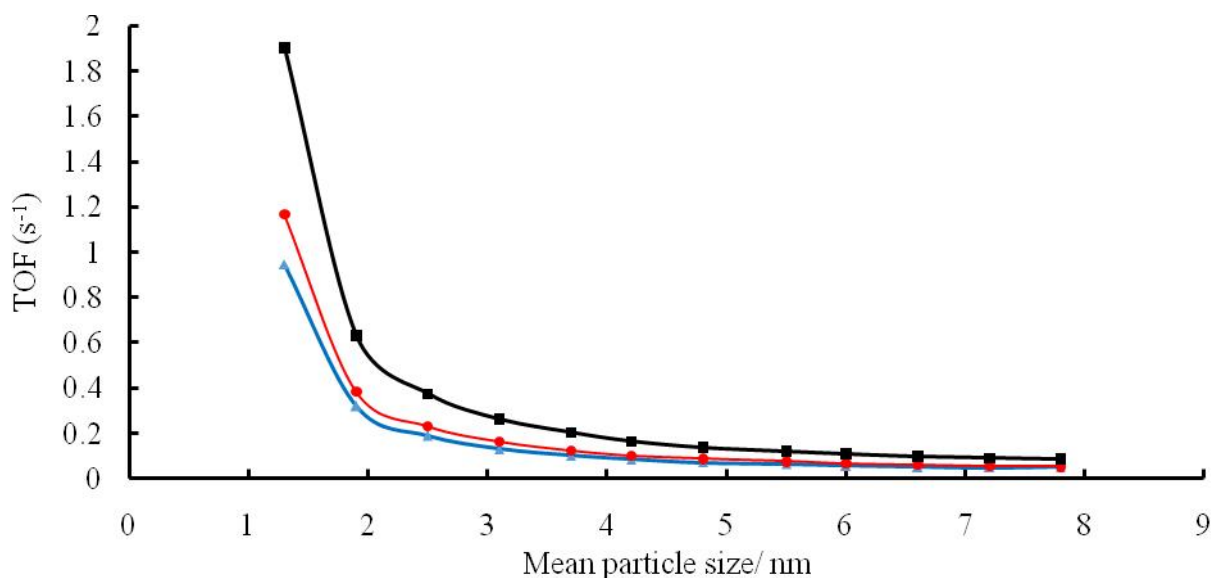

Figure 6: TOF for CO conversion on Pt particles catalyst for a pre-exposed CO Pt surface, pressure of 1.5 x 10^{-1} (blue triangles), 1.7 x 10^{-1} (red circles) and 2.2 x 10^{-1} mbar (black squires) at O$_2$: CO ratio of 1:2, 1:1 and 1:1, respectively, at 170 .

The TOF for CO conversion reaction at 240 with a pressure of 6 x 10^{-1}, 1.1 and 2.4 mbar at O_2: CO ratio of 1:1 is also presented, Figure 7.
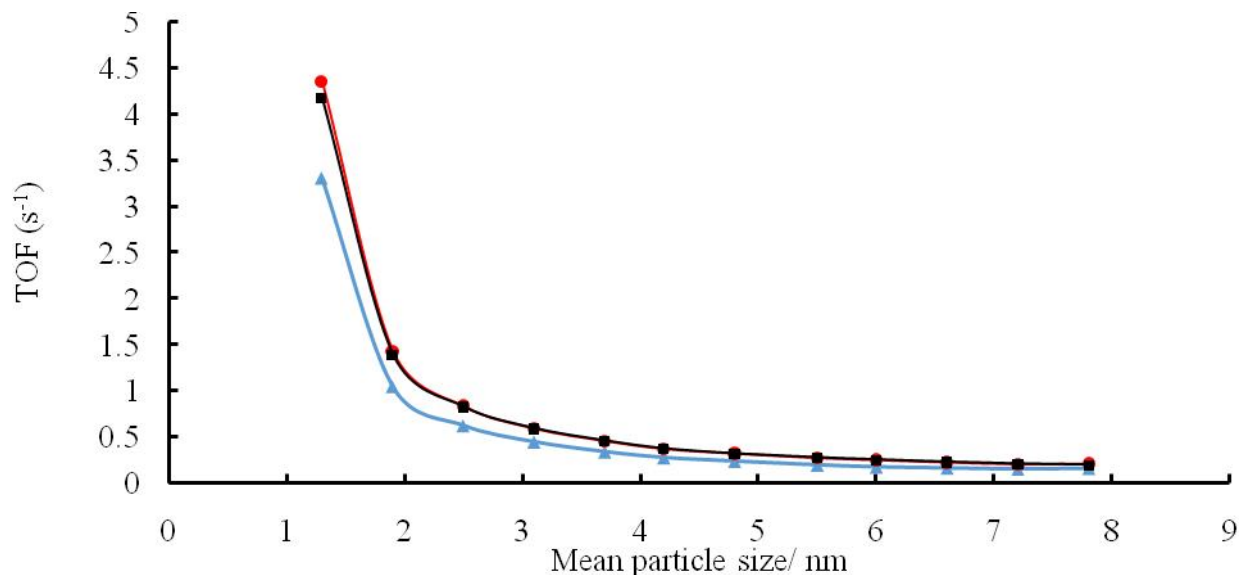

Figure 7: TOF for CO conversion on Pt particles catalyst at 240   and O_2: CO ratio of 1:1, pressure of 6.1 x 10^{-1} (blue triangles), 1.1 (red circles) and 2.4 mbar (black squires).

At each temperature, there is an increase in TOF as reactants pressures increase revealing that Pt catalyst is more active for CO conversion at higher pressure. For a pre-exposed O_2 catalyst surface at 170   , a similar trend in TOF of Pt catalyst was observed by increasing pressure, Figure 5. The same behaviour in TOF was noticed for a pre-exposed CO Pt catalyst surface at 170   , Figure 6. Again, reactants pressure led to a significant increase in activity of Pt catalyst for CO conversion with increasing pressure at 240   as shown by the values of TOF in Figure 7. Thus, the highest TOFs of Pt particles catalyst were achieved with increasing reactants pressure at higher temperature. Therefore, at each temperature, there is a linear relationship between the TOFs and pressure for CO conversion on Pt catalyst. The activity trend achieved in the current study is consistent with earlier findings which addressed the dependence on O_2 and CO pressure of the reaction rate for CO conversion on Pt catalysts (Li *et al*., 2013, Berlowitz *et al*., 1998). For a pre-adsorbed O_2 surface, TOF increased by raising CO pressure at O_2: CO ratio of 1:1, pressure of 2.2 x 10^{-1} mbar and on a Pt surface pre-adsorbed with CO, a similar trend was achieved, consistent with earlier reports (Berlowitz et al., 1998; Johanek *et al*., 2004; Li *et al*., 2013). TOF of Pt catalyst at 240   and higher reactant pressures resulted in the highest TOFs although a slight decline in activity was observed at 2.4 mbar, Figure 7. For example, TOF declined from 4.355 s^{-1} at 1.1 mbar to 4.174 s^{-1} at 2.4 mbar on Pt particle dimension of 1.3 nm. The fall of activity is attributed to CO inhibition of Pt catalyst surface

prohibiting O_2 adsorption and breakage on the catalyst surface, an important reaction pathway thus, decreasing Pt activity, in agreement with previous findings (McClure and Goodman, 2009). Results show that CO conversion on Pt catalyst is influenced by reactants pressure and surface temperature (Kolasinski:, 2002). For instance, at 170 and O_2: CO ratio of 1:1, Figure 4, TOF raised from 0.259 s^{-1} at 7.2 x 10^{-2} mbar to 1.991 s^{-1} at 1.04 x 10^{-1} mbar on Pt particle dimension of 1.3 nm. A similar raise in activity with increasing reactants pressure was attained on a pre-adsorbed O_2 Pt catalyst surface where TOF increased from 0.671 s^{-1} at 1.5 x 10^{-1} mbar to 1.889 s^{-1} at 2.2 x 10^{-1} mbar on Pt particle dimension of 1.3 nm, Figure 5. Besides, TOF increased from 0.946 s^{-1} at 1.5 x 10^{-1} mbar to 1.903 s^{-1} at 2.2 x 10^{-1} mbar on Pt particle dimension of 1.3 nm for a pre-adsorbed CO Pt surface, Figure 6. However, a competitive adsorption exists among CO and O_2 towards Pt surface, though CO can adsorb on an O_2 occupied surface, O_2 cannot adsorb on a CO occupied surface. Therefore, at high CO occupied surface, the reaction is restricted by O_2 thus, raising CO pressure prevents the reaction because there are no extra adsorption sites for O_2. Contrary, at low CO occupied surface, oxygen adsorption occurs rapidly and the reaction relies on the surface coverage of CO and O_2 (Kolasinski:, 2002). Usually, higher CO conversion to CO_2 is attained at situations that allow least CO surface occupancy (McClure and Goodman, 2009). In addition to temperature and pressure, CO conversion on Pt is dependent on particles dimension where the smallest particles exhibit higher activity. Although there is no common agreement from literature about the influence of particle dimension for supported Pt catalyst, results show that Pt particles within 1.1

nm and 10 nm, for CO conversion at different temperatures the activity increases with decreasing particle dimensions (Li et al., 2013). This is because for particle dimension of lower than 10 nm, the comparative number of kink sites, steps and corners raises monotonically with declining dimension and the low-coordinated surface atoms bare huge difference in the capability to react with molecules from the gas phase thus, accelerating the reaction (Overbury et al., 2006; Li et al., 2013). However, it is necessary to relate the activity trend with pressure at 170 and that attained at 240 . Results show higher activity of Pt catalyst at 240 as reflected in TOF with increasing pressure, for instance, TOF increased from 3.312 s^{-1} at 6.1 x 10^{-1} mbar to 4.355 s^{-1} at 1.1 mbar on Pt particle dimension of 1.3 nm. Studies show that Pt surface is exceptionally active at high reactant gas pressure and temperature because at low temperatures, the CO repressed regime takes over and the reaction is prohibited by adsorbed CO which preventing adsorption and breakage of O_2 thus, leading to low catalytic activity of Pt catalyst (Gao et al., 2009, McClure and Goodman, 2009, Liu et al., 2010). However, at all pressure and temperature conditions investigated in the current study, CO conversion rate increased with increasing pressure. Such activity trend illustrates the influence of pressure and temperature for CO conversion on Pt nanoparticles catalyst in addition to Pt particles dimension. This behaviour is consistent with earlier findings on the reliance of pressure of O_2 and CO of the reaction rate for CO conversion on a similar system (Berlowitz et al., 1998; Li et al., 2013). These result can be considered in the light of the influence of pressure to explain high activity of Pt catalyst at high pressure and temperature

among other factors (Li *et al*., 2013). The findings indicate that at a particular temperature, an increase of pressure yields the highest activity compared to that obtained at low pressure and temperature. Thus, these results provide the evidence of the influence of pressure on CO conversion on Pt particles catalyst at a given reaction temperature.

CONCLUSION

The CO conversion on titania supported Pt catalyst of different particle dimension between 1.3 nm and 7.8 nm at different reactants pressures was measured simultaneously on 120 catalysts at 170 and 240   and at different reactants pressures. The XPS studies indicated a small change of particle dimension after the reaction. At each temperature studied, a linear relationship between TOF for CO conversion on Pt catalyst and pressure was attained. However, the highest TOF for CO conversion on Pt was observed at higher pressure and temperature of 240   , consistent with earlier findings on similar catalyst system (Li *et al*., 2013, Berlowitz *et al*., 1998). However, a slight decline in activity was observed with a pressure of 2.4 mbar at 240   which is attributed to CO poisoning of Pt catalyst, consistence with earlier findings (McClure and Goodman, 2009). Besides, the smallest Pt particles attained the higher TOFs, in agreement with earlier reports.

Acknowledgement

References

Allian A.D., Kakanabe K., Fujdala K.L., Hao X.H., Truex T.J., Cai J., Buda C., Neurock M. and Iglesia E. 2011. Chemisorption of CO and Mechanism of CO Oxidation on Supported Platinum Nanoclusters. *J. Am. Chem. Soc.*. **133**(12): 4498-4517

Armor J.N. 2011. A history of industrial catalysis. Catalysis Today. 163: 3-9.

Attard G. and Barnes C. 1998. Surfaces, New York, Oxford University Press Inc.

Bamwenda G.R., Tsubota S., Nakamura T. and Haruta M. (1997). The influence of the preparation methods on the catalytic activity of platinum and gold supported on TiO_2 for CO oxidation. Catalysis Letters. 44: 83-87.

Berlowitz P. J., Peden C. H. F. and Goodman D. W. 1998. Kinetics of CO Oxidation on Single-Crystal Pd, Pt, and I r. *J. Phys. Chem*. **92**(18): 5213-5221.

Cameron, D., Holliday, R., Thompson, D. (2003). Gold's future role in fuel cell systems. *J. Power Sources* **118**(1-2): 298-303.

Dobrin S. 2012. CO oxidation on Pt nanoclusters, size and coverage effects: a density functional theory study. Physical Chemistry Chemical Physics. 14: 12122-12129.

Emmanuel J. 2022. Comparative activity of Platinum and Gold nanoparticles catalysts for Carbon monoxide oxidation. *Ethiop. J. Sci. Technol.* **15**: 155-172.

Emmanuel J. and Hayden B. 2022. Carbon Monoxide Oxidation on Model Planar Titania Supported Platinum Nanoparticles Catalyst. *Tanz. J. Sci.*. 48: 235-244.

Emmanuel J., Hayden B.E. and Saleh-Subaie J. 2019. The particle size dependence of CO oxidation on model planar titania supported gold catalysts measured by parallel thermographic imaging. *J. Catal*. **369**: 175-180.

Franceschetti A., Pennycook S.J. and Pantelides S.T. 2003. Oxygen chemisorption on Au nanoparticles. *Chem. Phys. Lett.*. **374**(5): 471-475.

Gao F., Wang Y., Cai Y. and Goodman D.W. 2009. CO Oxidation on Pt-Group Metals from Ultrahigh Vacuum to Near Atmospheric Pressures. 2. Palladium and Platinum. *J. Phys. Chem. C*. **113**(1): 174-181.

Guerin S., Hayden B.E., Pletcher D., Rendall M.E., Suchsland J.P. and Williams L.J. 2006. Combinatorial approach to the study of particle size effects in electrocatalysis: Synthesis of supported gold nanoparticles. *J. Comb. Chem.* **8**: 791-798.

Hannah L.M.V. 2012. The High Through-put Synthesis & Screening of Electrocatalysts for the Reduction of Nitrate in Groundwater and Waste Streams. Doctor of Philosophy, University of Southampton.

Haruta M. 2003. When Gold Is Not Noble: Catalysis by Nanoparticles. *Chem. Rec.* **3**: 75-87.

Hayden B.E. 2013. Particle Size and Support Effects in Electrocatalysis. *Acc. Chem. Res.* **46**: 1858-1866.

Hayden B.E., Pletcher D., Suchsland J.P. and Williams L.J. 2009. The influence of Pt particle size on the surface oxidation of titania supported platinum. *Phys. Chem. Chem. Phys.* **11**: 1564-1570.

Johanek V., Laurin M., Grant A.W., Kasemo B., Henry C.R. and Libuda J. 2004. Fluctuations and bistabilities on catalyst nanoparticles. *Sci.* **304**: 1639-1644.

Kageyama S., Sugano Y., Hamaguchi Y., Kugai J., Ohkubo Y., Seino S., Nakagawa T., Ichikawa S. and Yamamoto T.A. 2013. Pt/TiO2 composite nanoparticles synthesized by electron beam irradiation for preferential CO oxidation. *Mater. Res. Bull.* **48**(4): 1347-1351.

Kim G. and Jhi S.H. 2011. Carbon Monoxide-Tolerant Platinum Nanoparticle Catalysts on Defect-Engineered Graphene. *Acs Nano.* **5**: 805-810.

Kolasinski K.W. 2002. Surface Science: Foundation of Catalysis and Nanoscience, Queen Mary, University of London, UK, John Wiley & Sons, LTD.

Li N., Chen Q.Y., Luo L.F., Huang W.X., Luo M.F., Hu G.S. and Lu J.Q. 2013. Kinetic study and the effect of particle size on low temperature CO oxidation over Pt/TiO2 catalysts. *Appl. Catal. B: Environ.* **142**: 523-532.

Li S.Y., Liu G., Lian H.L., Jia M.J., Zhao G.M., Jiang D.Z. and Zhang W.X. 2008. Low-temperature CO oxidation over supported Pt catalysts prepared by colloid-deposition method. *Catal. Commun.* **9**: 1045-1049.

Liu C., Li G., Kauffman D.R., Pang G. and Jin R. 2014. Synthesis of ultrasmall platinum nanoparticles and structural relaxation. *J. Colloid Interface Sci.* **423**: 123-128.

Liu L. Q., Zhou F., Wang L.G., Qi X.J., Shi F., Deng Y.Q. 2010. Low-temperature CO oxidation over supported Pt, Pd catalysts: Particular role of FeOx support for oxygen supply during reactions. *J. Catal.* **274**: 1-10.

McCash E.M. 2001. Surface Chemistry, New York, Oxford University Press.

Mcclure S.M. and Goodman D.W. 2009. New insights into catalytic CO oxidation on Pt-group metals at elevated pressures. *Chem. Phys. Lett.* **469**(1): 1-13.

Molina L.M., Lesarri A. and Alonso J.A. 2009. New insights on the reaction mechanisms for CO oxidation on Au catalysts. *Chem. Phys. Lett.* **468**(4-6): 201-204.

Overbury S.H., Schwartz V., Mullim D.R., Yan W.F. and Dai S. 2006. Evaluation of the Au size effect: CO oxidation catalyzed by Au/TiO2. *J. Catal.* **241**: 56-65.

Rashkeev S.N., Lupini A.R., Overbury S.H., Pennycook S.J. and Pantelides S.T. 2007. Role of the nanoscale in catalytic CO oxidation by supported Au and Pt nanostructures. *Phys. Rev. B.* **76**(3): 035438.

Santos V.P., Carabineiro S.A.C., Tavares P.B., Pereira M.F.R., Orfao J.J.M. and Figueiredo J.L. 2010. Oxidation of CO, ethanol and toluene over TiO2 supported noble metal catalysts. *Appl. Catal. B: Environ.* **99**(1-2): 198-205.

Santra A.K. and Goodman D.W. 2002. Catalytic oxidation of CO by platinum group metals: from ultrahigh vacuum to elevated pressures. *Electrochim. Acta.* **47**: 3595-3609.

Scheidtmann J., Weiss P.A. and Maier W.F. 2001. Hunting for better catalysts and materials-combinatorial chemistry and high throughput technology. *Appl. Catal. A: Gen.* **222**(1-2): 79-89.

Schubert M.M., Hackenberg S., Van Veen A.C., Muhler M., Plzak V. and Behm R.J. 2001. CO oxidation over supported gold catalysts-"inert" and "active" support materials and their role for the oxygen supply during reaction. *J. Catal.* **197**: 113-122.

Slavinskaya E.M., Gulyaev R.V., Stonkus O.A., Zadesenets A.V., Plyusnin P.E., Shubin Y.V., Korenev S.V., Ivanova A.S., Zaikovskii V.I., Danilova I.G. and Boronin A.I. 2011. Low-temperature oxidation of carbon monoxide on Pd(Pt)/CeO2 catalysts prepared from complex salts. *Kinet. Catal.* **52**(2): 282-295.

Somorjai G.A. 1994. Introduction to Surface Chemistry and Catalysis, New York, John Wiley & Sons, Inc.

Zhang L., Persaud R. and Madey T.E. 1997. Ultrathin metal films on a metal oxide surface: Growth of Au on TiO2 (110). *Phys. Rev. B.* **56**: 10549-10557.

.